

DESIGN OF A NOVEL FLOW-AND-SHOOT MICROBEAM

G. Garty^{1,*}, M. Grad², B. K. Jones², Y. Xu¹, J. Xu^{2,3}, G. Randers-Pehrson¹, D. Attinger² and D. J. Brenner¹
¹RARAF, Columbia University, 136 S. Broadway, Irvington, NY 10533, USA

²Department of Mechanical Engineering, Columbia University, 500 W 120th Street, New York, NY 10027, USA

³Present address: Department of Mechanical Engineering, Washington State University, Vancouver, WA 98686, USA

*Corresponding author: gyg2101@columbia.edu

Presented here is a novel microbeam technology—the Flow-And-ShooT (FAST) microbeam—under development at RARAF. In this system, cells undergo controlled fluidic transport along a microfluidic channel intersecting the microbeam path. They are imaged and tracked in real-time, using a high-speed camera and dynamically targeted, using a magnetic Point and Shoot system. With the proposed FAST system, RARAF expects to reach a throughput of 100 000 cells per hour, which will allow increasing the throughput of experiments by at least one order of magnitude. The implementation of FAST will also allow the irradiation of non-adherent cells (e.g. lymphocytes), which is of great interest to many of the RARAF users. This study presents the design of a FAST microbeam and results of first tests of imaging and tracking as well as a discussion of the achievable throughput.

INTRODUCTION

Current microbeam systems⁽¹⁾ typically irradiate cells adhered to a thin membrane. The cells are mechanically moved to the location of the microbeam where they are individually targeted, either by a precision mechanical stage or by deflecting the beam slightly to hit individual cells (Point and Shoot). There are two drawbacks of this procedure. First, it only allows irradiation of cells that can be made to adhere to the membrane. Second, the positioning of the cells limits irradiation throughputs to about 10 000 cells per hour^(2, 3), limiting the possibility to probe rare endpoints such as mutagenesis and oncogenesis.

To expand irradiation throughput and capabilities, the authors propose to build a novel microbeam using Flow-And-ShooT (FAST) technology. In this system, cells will undergo controlled flow along a microfluidic channel intersecting the microbeam path. They will be imaged and tracked in real-time, using a high-speed camera and targeted for irradiation by single protons or helium nuclei, using the existing Point and Shoot system. With the proposed FAST system, a throughput of 100 000 cells per hour is expected, allowing experiments with much higher statistical power.

The implementation of FAST will also allow the irradiation of non-adherent cells (e.g. cells of hematopoietic origin), which is of great interest to many of the RARAF users. Current irradiation of lymphocytes is extremely difficult due to the low yield of cells that can be attached to a surface⁽⁴⁾.

Microfluidics overview

The term ‘microfluidics’ pertains to the behaviour, control and manipulation of fluids geometrically constrained to small length scales, where ‘micro’ forces such as surface tension overtake ‘macro’ forces such as gravity⁽⁵⁾. The field involves continuous flow microfluidics, which deals with the flow in channels with sub-millimetre critical dimensions, and digital microfluidics, which deals with nanolitre-to picolitre-sized droplets⁽⁶⁾. At these small length scales, viscous forces are much larger than inertia and the Reynolds number of the flow is very low ($Re \ll 1$). This leads to a laminar fluid flow that does not exhibit the random oscillations associated with the turbulent flow. Microfluidics is also naturally linked to biotechnology: continuous flow in microchannels can be used as a carrier for biological cells with high throughputs, and droplets can be used to encapsulate cells for isolation from external factors⁽⁷⁾. In this paper, we discuss both continuous flow (FAST microbeam) and digital microfluidics (cell encapsulation), and their impact on improvements to the microbeam at RARAF.

DESIGN OF THE FAST MICROBEAM

The FAST end station is designed for mounting on the Permanent Magnet Microbeam (PMM) at RARAF⁽⁸⁾. The PMM currently provides a focused He^{++} beam (5.2 MeV/5 μ m diameter/50–250 particles per second) with development under way for providing a proton microbeam (4.5 MeV/5 μ m).

The PMM is also equipped with a magnetic ‘Point and Shoot’ beam deflector, which can target the beam anywhere in a $60 \times 240 \mu\text{m}$ field-of-fire with a targeting time of < 1 ms.

The following three design criteria are important for designing a microfluidic channel for the microbeam system. First, a laminar flow pattern is sought; so the position of cells can easily be predicted. Second, the flow rate of the cells past the irradiation chamber must match the available beam flux. For example, given the $60\text{-}\mu\text{m}$ wide ‘field of fire’ of the Point and Shoot system and a beam flux of 100 particles per second, this translates into a required cell velocity of 6 mm s^{-1} to deliver a dose of 1 particle per cell. A proportionally slower velocity is required if multiple cells are present in the field-of-fire or if a higher dose is desired. Finally, the height of the channel and surrounding material must be limited; so it does not induce excessive beam scattering or prevent the beam from reaching the cells and the detector above the channels. This is not a problem for 4.5-MeV protons ($295\text{-}\mu\text{m}$ range in water) but is a significant limitation for 5.2-MeV helium nuclei ($40\text{-}\mu\text{m}$ range in water)

MANUFACTURING OF CHANNELS

The microfluidic channels used in this work were manufactured using soft lithography⁽⁹⁾. Since the channel width is larger than $100 \mu\text{m}$, moulds were made of polymethylmethacrylate (PMMA) slabs using a computer numerical controlled micromilling lathe (Minimill 3, Minitech Machinery). The accuracy of the lathe is between 2 and $5 \mu\text{m}$, with the surface roughness being on the order of 100 nm . Micro-endmills are commercially available with a diameter down to $25 \mu\text{m}$. The length scales of milled microgeometries ($50 \mu\text{m}$ to several millimetres) bridge the gap between the conventional macroscale machining (millimetre to metre) and lithography (nm to $100 \mu\text{m}$). The advantages of micromilling over UV lithography are that (1) a clean room is not required; (2) the cumbersome process of drawing and ordering photolithographic masks is replaced by the software generation of numerical commands to the milling machine out of a computer drawing and (3) the possibility to mill

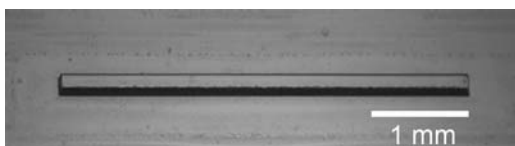


Figure 1. A mould for microchannel machined into PMMA using a micromilling machine.

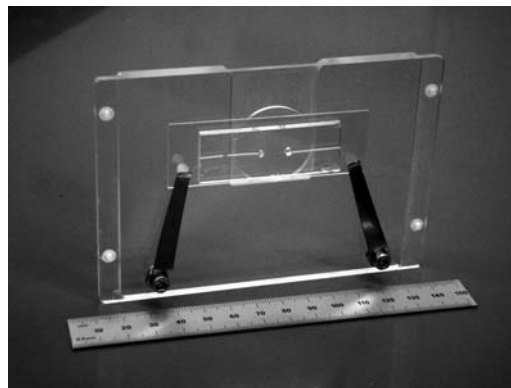


Figure 2. Photograph of flow-through chip used for testing cell tracking.

non-planar surfaces. A picture of a mould created with the micromilling machine is shown in Figure 1.

Once the mould is machined, Polydimethylsiloxane (PDMS)—a transparent silicone-based rubber—is poured over and allowed to harden to form three sides of the microfluidic channels. Both the PDMS and the planar surface used to seal the channel (made, for example, of glass, silicon, Si_3N_4 , mica) were treated with oxygen plasma for 30 s, and then permanently bonded together, as described elsewhere⁽⁹⁾.

For preliminary testing of cell flow and targeting, the authors have manufactured a PDMS microfluidic chip (Figure 2), featuring a flow-through channel, as described previously. For testing of the tracking system, the channels were sealed by plasma-bonding a standard glass cover slip. For cell irradiations, channels will be sealed to a $1\text{-}\mu\text{m}$ thick Si_3N_4 window, which will also serve as the beam-line vacuum window. The cross section of the channel has respective width and height of 200 and $20 \mu\text{m}$, so that the cells, when targeted by the microbeam, flow within $20 \mu\text{m}$ of the exit window. This should be contrasted with the distance of $50\text{--}100 \mu\text{m}$ currently maintained in the PMM between the exit window and the (moving) cell dish.

The flow rate is controlled by a syringe pump (KDS210, KD Scientific). Following irradiation, the cells will be either delivered into a capillary tube for storage or interfaced with other microfluidic chips (flow-through or cell dispensers) using modular polymeric connectors⁽¹⁰⁾.

CELL TRACKING

To perform single-cell-single-particle irradiation through the microfluidic channel, first, it is necessary to image and track the cells, and then shoot particle(s) at them. Due to geometry limitations of the

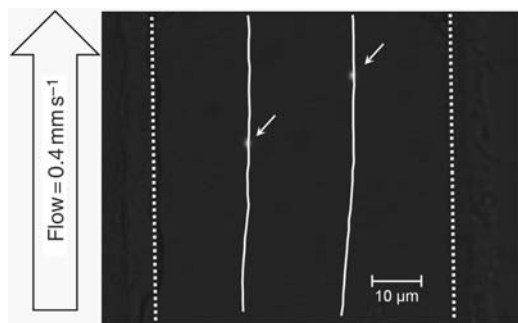


Figure 3. A fluorescent image of two beads flowing through a microfluidic channel. The beads are denoted by arrows, and the measured trajectories are overlaid. The dashed lines denote the boundaries of the channel.

microbeam end station, it is not possible to illuminate the sample from below. Consequently the RARAF microbeams have focused on epi-fluorescent imaging, using low concentrations of vital stains (e.g. Hoechst 33342). Epi-fluorescent imaging provides high-contrast images, enabling easy automation of the cell locating algorithm⁽³⁾. The beam size of $5\ \mu\text{m}$ and the typical target size (a lymphocyte nucleus is about $7\ \mu\text{m}$ in diameter) specify that a resolution of about $1\ \mu\text{m}$ per pixel is sufficient for tracking.

In their preliminary studies, the authors used a 25 frame-per-second (fps) image-intensified camera⁽³⁾ to take pictures of a fluorescent bead, then analysed the images and located its position at different times. In these experiments, the effective pixel size was $1.3\ \mu\text{m}$. Figure 3 shows an image of $5\ \mu\text{m}$ diameter fluorescent beads flowing through the channel. Because of the laminar flow, the bead motion is fairly smooth and linear⁽¹¹⁾, so that the cell position at subsequent time points can be accurately predicted. To determine the error in tracking, the authors:

- (1) Located all beads in each image (I_n), typically two to three beads,
- (2) Located, for each bead, the corresponding (closest) bead in the previous image (I_{n-1}).
- (3) Predicted, by linear extrapolation, the position of that bead in the next image (I_{n+1}).
- (4) Compared the position of the prediction with the actual position in the image I_{n+1} .

Figure 4 shows the distribution of prediction errors based on tracking 10 beads over 270 frames. More than 90 % of the errors are smaller than $1\ \mu\text{m}$ and 98 % are smaller than the $2.5\text{-}\mu\text{m}$ beam radius available in the PMM.

These experiments simulated an irradiation throughput of about 3000 cells per hour. To further increase the throughput, the authors are in the

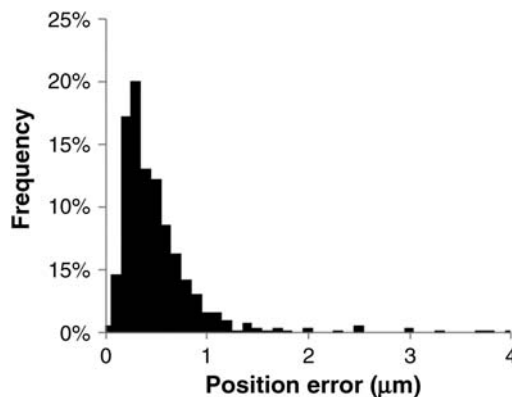


Figure 4. Error distribution of the predicted position.

process of incorporating a 30-times faster imaging based on a scientific CMOS camera⁽¹²⁾. The newly introduced sCMOS camera line combines high sensitivity with extremely fast data transfer rate (100 fps at 5 Megapixel and 900 fps at 320×240). The $6.5\ \mu\text{m}$ pixel size coupled with a $10\times$ objective will yield sufficient resolution for cell tracking, while covering the entire width of the channel even at a resolution of 320×240 . Preliminary tests using a prototype of the pco.edge, loaned to us by the Cooke Corporation, indicated its suitability for this application. Further tests will be performed when the commercial version becomes available in October 2010. The use of a fast camera along with the implementation of a hardware-accelerated tracking algorithm will allow both increasing of cell-flow speeds and flowing of a larger number of cells in parallel, with the aim of reaching an irradiation throughput of 100 000 cells per hour.

BEAM DELIVERY

Of prime importance in a microbeam system is the minimisation of beam scattering. This is achieved by the close proximity of the cells to be irradiated to the beam exit window. As noted above, the channel to be used is $20\ \mu\text{m}$ thick, with the accelerator exit window serving as its bottom surface. This constrains the cells to be within $20\ \mu\text{m}$ of the exit window, minimising the path of scattered particles to no more than $20\ \mu\text{m}$, during which they can only move a fraction of a micron laterally.

If necessary, in order to further push the cells down towards the irradiation window, the channel height can be locally reduced by incorporating a perpendicular pneumatic channel on top of the flow channel⁽¹³⁾; a constant pressure of about 100 mbar applied with a pressure regulator would force the

cells to pass in close contact with the irradiation window.

SRIM simulations of this geometry indicate a beam broadening of $<1\ \mu\text{m}$ at the top of the channel, due to scattering, for a He^{++} beam and negligible scattering for a proton beam. This will, of course, be verified using the standard knife edge technique⁽¹⁴⁾, using a TEM grid in the channel. By scanning the beam across the entire grid area and monitoring the residual beam energy as a function of targeted position, the authors can measure both the targeting accuracy and the spot size (the deflection required to transit between fully occluded and non-occluded).

In order to allow particle detection and counting, the chip was designed to be thin enough to be penetrated by 5-MeV He^{++} particles, with a residual energy of $>1\ \text{MeV}$ ($\sim 8\ \text{mm}$ range in air). This will allow the authors to couple the chip to a thin-window gas proportional counter, similar to the one the authors are currently using⁽³⁾ (this will, of course, not be an issue with the longer range protons).

INTEGRATION WITH OTHER TECHNOLOGIES

The addition of microfluidics into the microbeam end station offers additional flexibility for integrating the beam with other technologies, including cell sorting⁽¹⁵⁾ and cell encapsulation⁽¹⁶⁾.

Cell sorting

Currently, in microbeam systems, cell sorting is performed by manual cell manipulation with pipettes (at a speed of about 60 cells per hour). This process is very laborious and impractical, when dealing with larger numbers of cells. The integration of microfluidics into the microbeam end station allows for the easy integration of microfluidic cell sorters⁽¹⁵⁾. Sorting can take place before the irradiation, e.g. sorting cells by cell-cycle stage, to form a synchronised cell population for irradiation. Alternatively, cells can be sorted either immediately post-irradiation or cells can be irradiated and incubated together with normal cells before sorting, as required for bystander experiments⁽¹⁷⁾.

The authors have recently demonstrated⁽¹⁵⁾ manually controlled cell sorting at a rate of about 3000 cells per hour. By automating the cell recognition and switching, throughputs of 100 000 cells per hour are easily achievable.

Cell encapsulation

It has recently been shown that cells can be encapsulated in aqueous droplets submerged in microfluidic

channels filled with oil, isolating the cells from the surrounding environment in picolitre-volume ‘beakers’⁽⁶⁾. The encapsulation of cells in droplets can easily be integrated before the cells flow into the FAST microbeam, and the cells can be irradiated in the droplets as they flow past the microbeam. This technology has profound impacts on single-cell microbeams, because factors secreted by the cell during irradiation can be captured in a small volume and studied. Also, two or more cells can be encapsulated within the same droplet, one of which can be irradiated and kept in close proximity to the other cells. It is expected that, the bystander signal will be enhanced, due to the close proximity of the cells and the inability of secreted factors to diffuse away.

CONCLUSIONS

This study presents the preliminary design and testing of a novel microbeam technology under development at RARAF—the FAST microbeam. In this system, cells undergo controlled fluidic transport at rates of $1\text{--}10\ \text{mm}\ \text{s}^{-1}$ along a $200\text{-}\mu\text{m}$ -wide/ $20\text{-}\mu\text{m}$ -thick microfluidic channel intersecting the microbeam path. Cells are imaged and tracked in real-time, and dynamically targeted, using a magnetic Point and Shoot system. With the proposed FAST system, this study expects to reach a throughput of 100 000 cells per hour, which will allow increasing the throughput of microbeam experiments by at least one order of magnitude.

FUNDING

This work was supported by the national institute of biomedical imaging and bioengineering (NIH/NIBIB, grant #5P41EB002033).

REFERENCES

1. Bigelow, A. W., Brenner, D. J., Garty, G. and Randers-Pehrson, G. *Single-particle/single-cell ion microbeams as probes of biological mechanisms*. IEEE Trans. Plasma Sci. **36**, 1424–1431 (2008).
2. Bigelow, A., Garty, G., Funayama, T., Randers-Pehrson, G., Brenner, D. J. and Geard, C. *Expanding the question-answering potential of single-cell microbeams at RARAF, USA*. J. Radiat. Res. **50**, A21–A28 (2009).
3. Randers-Pehrson, G., Geard, C. R., Johnson, G., Elliston, C. D. and Brenner, D. J. *The Columbia University single-ion microbeam*. Radiat. Res. **156**, 210–214 (2001).
4. Kadhim, M. A., Marsden, S. J., Malcolmson, A. M., Folkard, M., Goodhead, D. T., Prise, K. M. and Michael, B. D. *Long-term genomic instability in human lymphocytes induced by single-particle irradiation*. Radiat. Res. **155**, 122–126 (2001).

FAST MICROBEAM

5. Stone, H. A., Stroock, A. D. and Ajdari, A. *Engineering flows in small devices*. *Annu. Rev. Fluid Mech.* **36**, 381–411 (2004).
6. Xu, J. and Attinger, D. *Drop on demand in a microfluidic chip*. *J. Micromech. Microeng.* **18**, (2008).
7. Berthier, J. and Silberzan, P. *Microfluidics for Biotechnology*. Artech House, Inc (2006).
8. Garty, G., Ross, G. J., Bigelow, A. W., Randers-Pehrson, G. and Brenner, D. J. *Testing the stand-alone microbeam at Columbia University*. *Radiat. Prot. Dosimetry* **122**, 292–296 (2006).
9. Xia, Y. and Whitesides, G. M. *Soft lithography*. *Annu. Rev. Mater. Sci.* **28**, 153–184 (1998).
10. Yuen, P. K. *SmartBuild-A truly plug-n-play modular microfluidic system*. *Lab Chip* **8**, 1374–1378 (2008).
11. Bruus, H. *Theoretical Microfluidics*. Oxford University Press (2008).
12. Holst, G. *Scientific CMOS imaging sensors: the new all-purpose imaging solution*. *Laser+Photonics* **2009**, 18–21 (2009).
13. Thorsen, T., Maerkl, S. J. and Quake, S. R. *Microfluidic large-scale integration*. *Science* **298**, 580–584 (2002).
14. Bigelow, A. W., Ross, G. J., Randers-Pehrson, G. and Brenner, D. J. *The Columbia University microbeam II endstation for cell imaging and irradiation*. *Nucl. Instrum. Methods Phys. Res. B* **231**, 202–206 (2005).
15. Grad, M., Jones, B., Smilenov, L., Brenner, D. and Attinger, D. *A Microfluidic Cell Sorter based on Hydrodynamic switching*. In: *Proceedings of International Mechanical Engineering Congress and Exposition, Orlando (2009)*.
16. Xu, J. and Attinger, D. *Dispensing individual fluid particles on demand in a microfluidic chip*. *Proceedings of MicroTAS, San Diego*, pp. 1378–1380 (2008).
17. Hei, T. K., Zhou, H., Ivanov, V. N., Hong, M., Lieberman, H. B., Brenner, D. J., Amundson, S. A. and Geard, C. R. *Mechanism of radiation-induced bystander effects: A unifying model*. *J. Pharm. Pharmacol.* **60**, 943–950 (2008).